Desalination and Water Treatment
www.deswater.com

doi: 10.1080/19443994.2016.1167126

57 (2016) 27048–27060
December

Taylor & Francis
Taylor & Francis Group

Evaporation process for treating high-salinity industrial wastewater at low temperatures and ambient pressure

Haoming Li[a], Heli Wang[a,*], Qingsong Liu[a], Yao Tan[b], Nan Jiang[c], Yingzi Lin[d]

[a]*School of Water Resources and Environment, China University of Geosciences, Beijing 100083, China, email: lhm68005@163.com (H. Li), Tel. +86 13801275897; Fax: +86 10 82320987; emails: wangheli@cugb.edu.cn (H. Wang), liukingsong@163.com (Q. Liu)*
[b]*Department of Research and Development, Creative Water Technology China, Ltd. Co., Beijing 100102, China, email: Yao-tan@hotmail.com*
[c]*International College of Beijing University of Agriculture, Beijing University of Agriculture, Beijing 100022, China, email: jiangnan_cugb@126.com*
[d]*School of Environmental and Municipal Engineering, Jilin Jianzhu University, Changchun 130118, China, email: linyingzi1000@163.com*

Received 15 November 2015; Accepted 13 March 2016

ABSTRACT

High-salinity industrial wastewater is difficult to treat. In this study, an evaporation process for use in cooling towers and seawater desalination was adapted to treating high-salinity wastewater under gentle operating conditions. Real wastewater and simulated wastewater containing sodium chloride and glucose were used in this study. An evaporation unit, with an evaporation rate of 5 L/h, was designed and installed in the laboratory. Analysis revealed the effects of operating factors on the quality of condensed water, as well as the relationship between the mass transfer coefficient and wastewater characteristics. The results showed that for the selected system, when the inlet air speed was below 2.5 m/s and the wastewater flow rate was below 1.0 m^3/h, the total dissolved solids and the chemical oxygen demand removal efficiencies could reach up to 99.9%. The most significant difference between the mass transfer coefficients of the clean water and simulated wastewater was 30.9% under identical operating conditions. The equation of the mass transfer coefficient considering the density, viscosity, and saturated vapor pressure of wastewater was built to predict the mass transfer efficiency for this process. A case study using real wastewater from a pharmaceutical factory illustrated that the system performed well in practical situations. The predicted mass transfer coefficient agreed well with the measured value. In summary, the developed evaporation system has good prospects for the treatment of high-salinity industrial wastewater.

Keywords: Wastewater treatment; Evaporation; Low temperature and ambient pressure; Mass transfer coefficient; Wastewater characteristics

*Corresponding author.

1. Introduction

Industrial wastewater is generated from numerous industries and is generally difficult to treat. For example, during the production of glyphosate, 5–6 tons of high-salinity wastewater is produced to obtain 1 ton of glyphosate [1]. High-salinity wastewater contains highly concentrated organics and dissolved salt that are poisonous to the micro-organisms used for biotreatment. The discharge of high-salinity wastewater without treatment is harmful to the environment and human health [2–4]. Although the application of salt-tolerant bacteria for biological treatment has been studied to improve the efficiency of high-salinity wastewater treatment, this research remains in its early stage. In recent years, high-salinity wastewater has typically been treated using physical and chemical methods, such as evaporation techniques and membranes filtration. Among these methods, the evaporation techniques have great potential for wastewater treatment because they are easy to use and perform well [5].

Currently, various types of evaporation techniques, such as multi-effect distillation (MED), mechanical vapor recompression (MVR), adsorption desalination (AD), multi-stage flash (MSF), and membrane distillation (MD), are used for treating high-salinity wastewater. Among these techniques, MED and MVR are considered more effective than MSF and MD [5–7]. The applications of MED have had great success for seawater desalination and industrial wastewater treatment [8–10]. MVR has also been used in thousands of facilities for seawater desalination and industrial wastewater treatment around the world [11]. AD is an emerging thermally driven desalination process, with a low energy cost that is suitable for treating wastewater with salinities of up to 250,000 ppm [12–14]. However, the use of AD at large scales requires time.

The traditional evaporation techniques (e.g. MED and MVR) used for wastewater treatment are processes of mass and heat transfer at constant temperature. In such processes, the wastewater is evaporated at low temperatures and negative pressures. Recently, an evaporation process based on direct contact heat and mass transfer between water and air has been examined. This process simulates the evaporation of precipitation, and does not involve boiling the water. Compared with other evaporation techniques, a significant advantage of this evaporation technique is that the direct contact between water and air allows wastewater evaporation at low temperatures and ambient pressures, resulting in easy system installation and operation. Hence, valuable commodities in the wastewater that are heat sensitive could be separated and recycled using this evaporation technique. Additionally, low-temperature and ambient-pressure operation allows the use of mostly non-metal materials, which prevent scaling [15,16].

Some analyses of the evaporation processes based on direct contact between water and air have been performed. However, most investigations have focused on seawater desalination and cooling towers. Klausner et al. [17] investigated an analytical model providing a general approach to predict the evaporative heat and mass transfer phenomena for a diffusion-driven desalination process with different liquid/air fluxes. Lemouari et al. [18] investigated the effects of the air and water flow rates on the heat and mass transfer coefficients and the evaporation rate of water into the air stream for different inlet water temperatures. Bourouni et al. [19] and Al-Hallaj et al. [20] reported the operation of HDH units in Tunisia and Jordan, respectively. For all of the above studies, clean water or seawater was used as the study medium, while the characteristics of the water were invariant. These studies mainly focused on the effects of operating conditions and the parameters of the evaporator and fillers on the evaporation rates.

Few studies have described the application of the evaporation processes based on direct contact between water and air for treating high-salinity industrial wastewater. This type of evaporation process is different than that used for seawater desalination and in cooling tower, because wastewater contains various impurities. Moreover, the quality of the condensed water needs to be considered, since it must meet discharge standards. In addition to other factors, the salinity of high-salinity wastewater varies widely and strongly influences the treatment performance of the evaporation process for wastewater treatment. However, the exact influences of salt concentration have not been reported.

In this study, a low-temperature and ambient-pressure evaporation system for treating high-salinity industrial wastewater was investigated. The objectives of this study were as follow: (1) to set up an evaporation system applicable for the treatment of high-salinity industrial wastewater based on direct contact between wastewater and air at low temperature and ambient pressure; (2) to elucidate the effects of operating factors, including the temperature of the inlet wastewater, the speed of the inlet air, and the flow rate of the inlet wastewater, on the quality of condensed water; and (3) to illustrate the relationship between the mass transfer coefficient and various wastewater characteristics.

2. Materials and methods

2.1. Wastewater samples

Simulated wastewater with various sodium chloride (>1%) and glucose concentrations was used to examine the treatment effects and evaporation rates in a pilot study. Clean water was used as a blank. For the case study, both simulated wastewater and real pharmaceutical wastewater were tested. Simulated wastewater in the case study was also prepared with sodium chloride and glucose, and the values of total dissolved solids (TDS) and chemical oxygen demand (COD) were close to the real wastewater used in case study. Detailed concentrations of TDS and COD in wastewater samples are listed in Table 1.

2.2. Evaporation system configuration

A lab-scale unit of a direct contact evaporation system with a capacity of 5 L/h (evaporation rate) was designed and installed in the laboratory. As shown in Fig. 1, this system consisted of an evaporation chamber, a cooling chamber, a heating section, and an air pipe. The evaporation chamber had dimensions of 350 mm × 350 mm × 800 mm and represented the main device used in the test. The packing had a cross-sectional test area of 320 mm × 320 mm, a height of 360 mm, and a specific surface area of 200 m^2/m^3. The packing was organized as a group of PVC plates, similar to that used in a cooling tower. The distance between two plates was 6 mm. In the top of the evaporation chamber, a group of eliminators with a multi-arc frame and dimensions of 320 mm × 320 mm × 150 mm was used to trap the entrained droplets and return them to the packing zone. At the bottom of the evaporation chamber, a centrifuge separator was used to obtain solids from the concentrated liquid. A 5.5-kW electric heater was used in the heating section. A circulation pump fed the water at a maximum flow rate of 3.0 m^3/h. In the air pipe, a fan was used to create air flow with a maximum flow rate of 5.5 m/s. The cooling chamber had the same dimensions as the evaporation chamber. In the cooling chamber, a cooler coil with a surface area of 155 m^2 served as the condenser. Tap water was used as the cooling water. Auxiliary devices were also attached, such as thermometers, humidity meters, and flow rate controllers for the air and wastewater.

Wastewater was pumped from the heating section by circulation pump as the feed water and uniformly sprayed over the packing in the top of the evaporation chamber. Low-humidity air was introduced by a fan at the bottom of the evaporation chamber. As the wastewater passed through the packing and was exposed countercurrently to the air flow, a thin film of water was formed on the surface of each filler plate in direct contact with the low-humidity air. As dictated by the conservation of mass, momentum, and energy, liquid water would evaporate and be transferred into the air because of concentration gradients. During this process, the wastewater was concentrated and cooled by evaporation, and the air moisture content increased. The concentrated and cooled wastewater moved to the bottom of the evaporation chamber and was mixed with recharge wastewater in the heating section for further evaporation until supersaturation. In this study, for each sample, the condensed water was used as recharge water to keep a constant salt concentration. The recrystallized salts were separated from the concentrated water through the separator at the bottom of the evaporation chamber. Upon leaving the top of the chamber, the saturated air passed through the drift eliminator to the cooling chamber, where the water vapor was condensed into liquid (discharge water). The saturated air was turned to low-humidity air and recirculated into the evaporation chamber.

Table 1
Concentrations of TDS and COD in wastewater

No. of sample	TDS (mg/L)	COD (mg/L)
1	0	0
2	31,825	7,200
3	49,178	15,710
4	66,732	21,330
5	81,070	27,400
6	89,177	20,800
7	104,051	31,700
8	114,905	42,200
9	124,955	43,900
10	133,330	48,800
11	135,876	53,600
12	140,365	58,300
13	148,740	61,300
14	151,420	61,400
15	154,770	65,100
16	155,105	70,700
17	155,440	77,100
18	155,775	75,300
19	157,584	79,100
20	159,460	80,000
21	162,475	133,100
22[a]	110,952	32,500
Pharmaceutical wastewater	107,401	43,800

[a]Sample no. 22 was used in the case study.

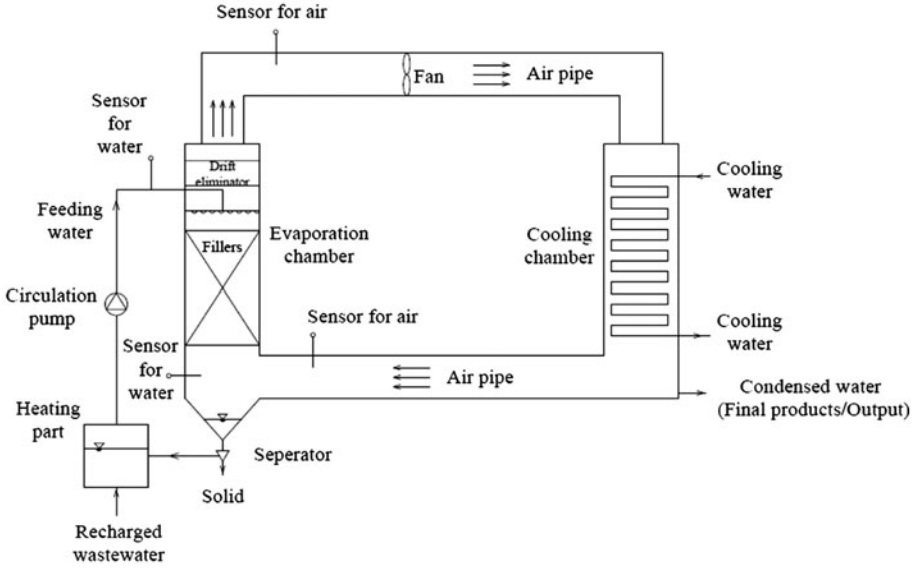

Fig. 1. Schematic diagram of the evaporation system.

2.3. Experimental procedure

To investigate the treatment effects under different operating conditions, simulated wastewater with 162,475 mg/L TDS and 133,100 mg/L COD was used as the study medium. The controllable operating factors of the developed evaporation system for wastewater treatment included the temperature of the inlet wastewater and the flow rates of the inlet wastewater and inlet air speed. Inlet air speed varied from 1.5 to 5.5 m/s with a step size of 1 m/s for each wastewater flow rate (0.5, 1.0, 1.5, 2.0, and 2.5 m^3/h). The experiments were repeated at the inlet water temperature of 40, 50 and 60°C, respectively. Condensed water was analyzed for TDS and COD.

To determine the evaporation rates of wastewaters with different salt concentrations, simulated water no. 1–21 (Table 1) were used as the study media. The inlet wastewater flow rate, air flow rate, and inlet wastewater temperature were 1.0 m^3/h, 2.5 m/s, and 60°C, respectively. The properties of the wastewater and air were determined for temperature and humidity in the system. Wastewater was measured for the specific heat, density, saturated vapor pressure, and viscosity, respectively.

In the case study, the inlet wastewater flow rate, air flow rate, and temperature of the inlet wastewater were 1.0 m^3/h, 2.5 m/s, and 60°C, respectively.

2.4. Process modeling in the evaporation chamber

Fig. 2 shows the heat and mass transfer processes between the liquid and gas in the evaporation chamber. The evaporation process facilitated the heat and mass transfer between the water and air via convection through direct contact with each other on the surface of the filler.

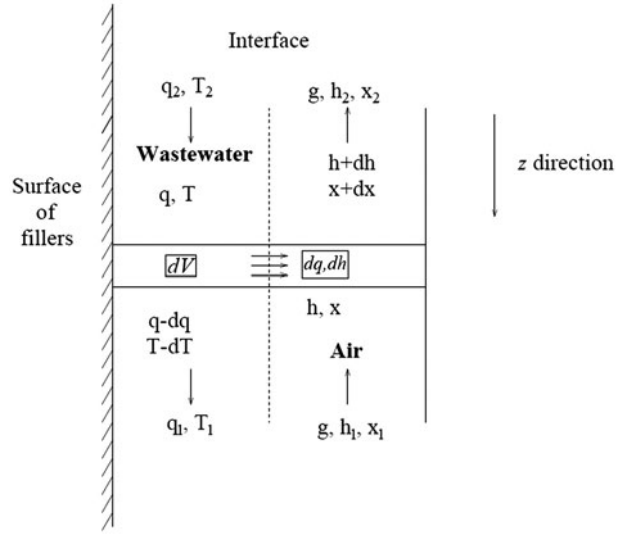

Fig. 2. Heat and mass transfer between wastewater and air in the evaporation chamber.

The following assumptions were applied for modeling:

(1) The system was in a steady state.
(2) No heat or mass transfer occurred between the system and the environment, and the energy loss during the process was negligible.

(3) The temperature and humidity of air only changed in the z direction.
(4) For all fillers, the water and air contact time was sufficient for the heat and mass transfer on the interface.
(5) The mass transfer area and heat transfer area were equal.
(6) The mass flow rates of the wastewater and air were stable in their flow directions.

The specific heat, temperature, and mass flow rate of the wastewater are represented by c_w, T, and q, respectively. The mass flow rate of the air is represented by g. The enthalpies of the inlet and outlet air are indicated by h_1 and h_2, respectively. The humidities of the inlet and outlet air are represented by x_1 and x_2, respectively. β_{xv} is the volumetric mass transfer coefficient. A micro unit dV in Fig. 2 was taken as the system in the modeling.

According to the mass balance:

$$dq = g \cdot dx = \beta_{xv} \cdot (x_2 - x_1)\, dV \tag{1}$$

According to the heat balance:

$$d(c_w q T) = g \cdot dh = \beta_{xv} \cdot (h_2 - h_1)\, dV \tag{2}$$

The Lewis relation is as follows:

$$Le_c = \frac{\alpha}{\beta_{xv}(c_a - c_v x)} \tag{3}$$

Eq. (3) is a precondition for Eq. (2). According to the empirical calculation, the Lewis number (Le_c) reflects the relationship between the heat transfer and the mass transfer between liquid and gas and $Le_c = 1$.

Due to the complexity of the mass transfer process, it is challenging to investigate the entire mass transfer unit. Therefore, only the mass transfer of the micro unit was assessed. Under this condition, the volumetric mass transfer coefficient β_{xv} indicates the evaporation rate.

Based on Eqs. (1) and (2) and the Merkel method, the heat and mass transfer data are correlated with the following equation [21]:

$$\beta_{xv} \cdot (h_2 - h_1) \cdot S \cdot dZ = \frac{1}{K} \cdot c_w \cdot q \cdot dT \tag{4}$$

Integrating Eq. (4), β_{xv} can be calculated as follows:

$$\beta_{xv} = \frac{c_w \cdot q \cdot (T_2 - T_1)}{K \cdot V} \cdot \frac{1}{6} \cdot \left(\frac{1}{h'_2 - h_1} + \frac{4}{h'_m - h_m} + \frac{1}{h'_1 - h_2} \right) \tag{5}$$

where T_2 and T_1 are the temperatures of the inlet and return water in the evaporation chamber, respectively. h'_1 and h'_2 are the enthalpies of the saturated air at the temperatures of the input and return water, respectively. h_m is the average value of h_1 and h_2. h'_m is the average value of h'_1 and h'_2. K is the correction factor of the evaporated water quantity. K is calculated using the following equation:

$$K = 1 - \frac{c_w \cdot T}{r(T)} \tag{6}$$

where $r(T)$ is the latent heat of wastewater vaporization when the temperature is T.

Here, β_{xv} is determined from experimentally testing the air and water parameters (e.g. temperature, humidity, and enthalpy). The evaporation rate is determined by analyzing the mass and heat transfers. The intrinsic influencing factors of β_{xv} need to be further investigated (e.g. the movement behavior of the wastewater, the characteristic parameters of the evaporator, and the physical and chemical properties of the wastewater).

As shown in Fig. 2, the evaporation process consists of the heat and mass transfer between the water and air via convection. Based on the similarity of the convective mass transfer:

$$S_h = A S_c^B \, Re^C \left(\frac{L}{Z} \right)^D \tag{7}$$

where S_h is the Sherwood number that includes the mass transfer coefficient and reflects the correlation between the mass transfers of convection and diffusion as follows:

$$S_h = \beta_P \cdot \frac{L}{D_P} \tag{8}$$

S_c is the Schmidt number that describes the momentum diffusion and mass diffusion of a fluid:

$$S_c = \mu \cdot (D_P \cdot R_{ws} \cdot T \cdot \rho)^{-1} \tag{9}$$

Re is the Reynolds number that represents the movement behavior of a fluid:

$$Re = U \cdot L \cdot \rho \cdot \mu^{-1} \tag{10}$$

L/Z is the characteristic size of the filler.

R_{ws} is the vapor gas constant.

β_P is the area mass transfer coefficient based on the pressure difference:

$$\beta_P = 0.622\frac{\beta_{xv}}{a'P} \tag{11}$$

where a' is the specific surface area of the packing, and P is the saturated vapor pressure of the wastewater.

D_P is the diffusion coefficient based on the pressure difference:

$$D_P = \frac{6.27\times10^{-8}}{P}\cdot\left(\frac{T}{273.15}\right)^{0.8} \tag{12}$$

where T is the wastewater temperature.

U is the relative velocity between the air and wastewater:

$$U = U_L + U_W = \frac{G}{S-ndL} + \sqrt{[3]}\frac{1}{3\mu\rho}\cdot\left(\frac{q_w}{3.6\cdot a'}\right)^2 \tag{13}$$

where U_L and U_W are the velocities of the air and wastewater, respectively. G is the volumetric flow rate/cross-sectional area of the air. n is the number of filler plates. d is the distance between two plates. q_w is the flow rate of the wastewater. μ and ρ are the viscosity and density of the wastewater, respectively.

Thus, Eq. (7) is expressed as follows:

$$0.622\frac{\beta_{xv}}{a'P}\cdot\frac{L}{D_P} = A\left(\frac{\mu}{D_P\cdot R_{ws}\cdot T\cdot\rho}\right)^B\left(\frac{U\cdot L\cdot\rho}{\mu}\right)^C\left(\frac{L}{Z}\right)^D \tag{14}$$

In Eq. (14), A, B, C, and D are unknown constants. According to Eq. (14), the volumetric mass transfer coefficient is related to the density, viscosity, and saturated vapor pressure of the wastewater when the other operating conditions are unchanged.

2.5. Analytical methods

TDS was determined by a portable detector (HQ40d, HACH, USA). COD was measured with an ultraviolet spectrophotometer (DR 2800, HACH, USA) according to standard methods. The wastewater specific heat was analyzed by the differential scanning calorimeter method. The density of the wastewater was measured by a densitometer. The saturated vapor pressure of the wastewater was analyzed by the steady-state method. The viscosity of wastewater was measured by a ball viscometer using a standard method.

3. Results and discussion

Wastewater was separated into concentrated liquid and condensed water through the evaporation process. The condensed water was discharged when it met the emission standards. The concentrated liquid was pumped into the heating section by a screw pump for further evaporation cycling until solid precipitation was achieved. The recharged wastewater was mixed with the concentrated liquid in the heating section to guarantee flow in the pipe. Thus, the final products obtained using continuously fed wastewater were solid and condensed water (discharge water). The recrystallized salts obtained from the separator at the bottom of the evaporation chamber had 15.6% moisture content. These salts were then disposed of sanitarily or purified for recovery.

3.1. Effects of operating factors on the evaporation treatment

As the inlet wastewater temperature increased from 40 to 60°C, the TDS and COD removal efficiencies of the wastewater remained similar under the same inlet wastewater and air flow rates. In this temperature range, the TDS and COD removal efficiencies were all nearly 99.9% when the inlet wastewater flow rate was 1.0 m^3/h and air speed was 2.5 m/s. Thus, the inlet water temperature had little effect on TDS and COD removal via evaporation from high-salinity and nonvolatile organic wastewater. The processes of heat and mass transfer for evaporation in this study and cooling tower are similar. Therefore, the operating conditions used for the process in cooling towers could serve as a reference. Based on the previous results from cooling towers [18,22,23], high evaporation rates could be achieved at high inlet water temperatures. Thus, an inlet wastewater temperature of 60°C was chosen in this study for the developed evaporator.

The TDS and COD significantly decreased in the condensed water after evaporation. The removal efficiencies of TDS and COD were at least 86.4% and up to 99.9%, respectively (Fig. 3). The TDS and COD removal efficiencies were stable and relatively high when the inlet air speed was below 2.5 m/s for each wastewater flow rate. The removal efficiencies decreased when the inlet air speed was increased to more than 2.5 m/s. The main reason for the decrease

was that in the top of the evaporation chamber, when the air speed increased to the critical level, the eliminator had difficulty capturing the small-sized wastewater droplets because of the turbulent air. Large-sized droplets with greater momentum were contained in the air and were broken into small droplets or splashed while passing through the eliminator. Thus, the liquid entrainment increased, and more wastewater droplets passed through the eliminator and were mixed with the condensed water, which decreased the quality of the condensed water.

When the wastewater flow rate increased to 1.0 m^3/h, for inlet air speeds of 1.5 m/s and 2.5 m/s, the removal efficiencies of TDS and COD exhibited little change (Fig. 3). The efficiencies deceased more noticeably when the wastewater flow rate increased greater than 1.5 m^3/h and the inlet air flow rate exceeded 2.5 m/s. The wastewater was splashed more violently when the water flow rate increased, and more droplets were carried to the eliminator. The problem of liquid entrainment could be somewhat overcome by maintaining the inlet air speed at less than 2.5 m/s; however, the eliminator was overloaded when the inlet air speed exceeded 2.5 m/s for high wastewater flow rate.

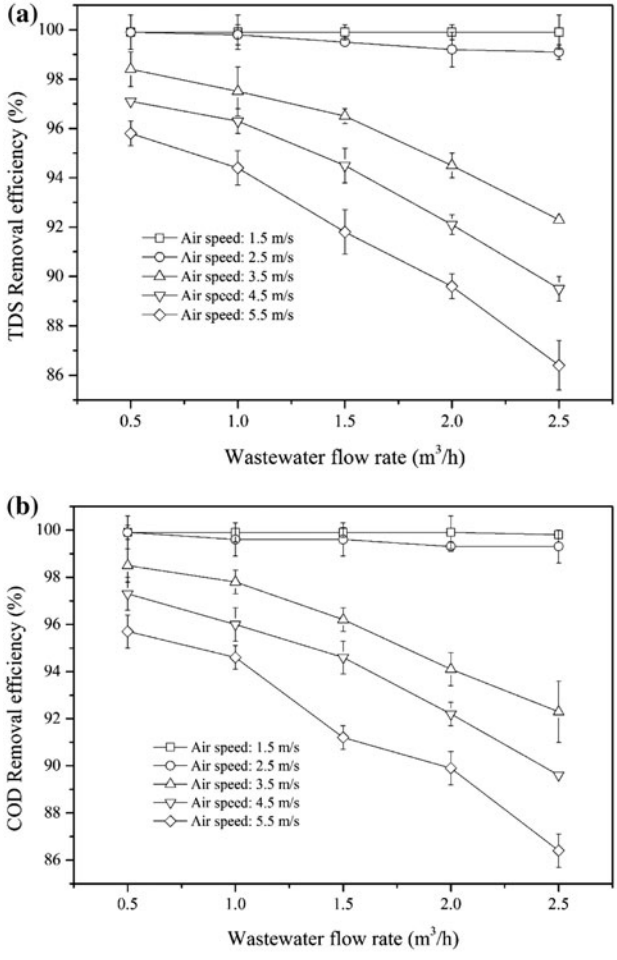

Fig. 3. Removal of TDS and COD under different wastewater flow rates and air speeds at 60℃.

The problem of liquid entrainment has also been reported in cooling tower studies measuring the water losses [24,25]. Thus, for the selected evaporator and eliminator, the operating conditions must be controlled to reduce the liquid entrainment and ensure the production of high-quality condensed water. Based on the test results from the previous studies of cooling towers [18,22,23] and the results obtained using the evaporator in this study, an inlet air flow of 2.5 m/s, an inlet water flow of 1.0 m^3/h, and an inlet water temperature of 60℃ were chosen to achieve rapid evaporation and high-quality condensed water.

The treatment effects for wastewaters with different salt concentrations were also tested using the operating conditions listed above, and the results are shown in Table 2. The TDS and COD removal efficiencies for these samples were all nearly 99.9%. The developed evaporator exhibited good performance for treating wastewater with different salt concentrations.

MED and MVR have been successfully applied for industrial wastewater treatment [8–11]. However, a high risk of scaling/blocking in the evaporator was reported during their testing [26], which did not occur in this study. The wastewater in the evaporator likely boiled easily under negative pressure when using MED and MVR, and the evaporation process is violent. In this study, wastewater was gently evaporated at low temperature and ambient pressure, and the salts or other solids in the wastewater were removed by the separator at the bottom of the evaporation chamber. Thus, the risk of scaling/blocking was significantly reduced. For seawater or industrial wastewater with high concentrations of dissolved salts that cause scaling, pretreatment is necessary to prevent scaling, which could include physical adsorption and the addition of chemical agents, etc. [27].

3.2. Effects of salinity on evaporation rates

Although the mass and heat transfer processes have been studied in cooling towers and seawater desalination, they would differ in wastewater treatment. According to Eq. (14), the physical and chemical properties of the wastewater significantly affect the evaporation rate.

The experimentally determined properties of the wastewater and air are shown in Table 3. Using Eq. (5) and the data in Table 3, the value of β_{xv} was

Table 2
TDS and COD removal efficiencies for wastewater samples

No. of sample	TDS			COD		
	Inlet (mg/L)	Condensed water (mg/L)	Removal efficiency (%)	Inlet (mg/L)	Condensed water (mg/L)	Removal efficiency (%)
1	0	0	–	0	0	–
2	31,825	38	99.9	7,200	30	99.6
3	49,178	44	99.9	15,710	26	99.8
4	66,732	57	99.9	21,330	46	99.8
5	81,070	67	99.9	27,400	81	99.7
6	89,177	75	99.9	20,800	53	99.8
7	104,051	67	99.9	31,700	47	99.9
8	114,905	96	99.9	42,200	62	99.9
9	124,955	89	99.9	43,900	62	99.9
10	133,330	103	99.9	48,800	55	99.8
11	135,876	99	99.9	53,600	64	99.9
12	140,365	96	99.9	58,300	37	99.9
13	148,740	102	99.9	61,300	55	99.9
14	151,420	67	99.9	61,400	49	99.8
15	154,770	97	99.9	65,100	66	99.8
16	155,105	88	99.9	70,700	80	99.9
17	155,440	102	99.9	77,100	75	99.9
18	155,775	90	99.9	75,300	60	99.9
19	157,584	102	99.9	79,100	90	99.8
20	159,460	101	99.9	80,000	89	99.9
21	162,475	102	99.9	133,100	93	99.8
22[a]	110,952	67	99.9	32,500	61	99.8
Pharmaceutical wastewater	107,401	63	99.9	43,800	1,823	95.8

Notes: Operation conditions: 2.5 m/s of inlet air flow, 1.0 m^3/h of inlet water flow and an inlet water temperature of 60°C.
[a]Sample no. 22 was used in the case study.

calculated for all of the experiments and is presented in Table 4. Here, β_{xv} was determined by analyzing the process of the mass and heat transfers. Intrinsically, the factors leading to different β_{xv} values were the density, viscosity, and saturated vapor pressure of the wastewater.

For samples no. 1–21, the density increased from 1,000.0 to 1,215.7 kg/m^3 and the viscosity increased from 0.4688 to 1.7590 mPa s. The saturated vapor pressure decreased from 19.90 to 15.01 kPa (Table 5).

The volumetric mass transfer coefficient (β_{xv}) decreased from 3,197.70 to 2,209.42 kg/(m^3 h) as the salt concentration in the wastewater increased, as shown in Table 4. The greatest significant difference in β_{xv} between clean water and high-salinity wastewater was 30.9%. There were two main reasons for this phenomenon. (1) The partial pressure of the steam and the temperature gradients between the water and air were the direct driving forces of the heat and mass transfer processes during evaporation. Combining these two factors, the driving force identified to be an enthalpy difference, as shown in Eq. (4). Therefore, the evaporation speed was directly affected by the saturated vapor pressure. During the experiments, the saturated vapor pressure of the wastewater decreased from 19.90 to 15.01 kPa, thereby decreasing the driving force. (2) The evaporation process consisted of the heat and mass transfers occurring during direct contact of the counter-flowing wastewater and air. According to Eq. (14), the factors that influenced the wastewater and air flow also affected the evaporation rate. During the experiments, the wastewater density and viscosity increased from 1,000.0 to 1,215.7 kg/m^3 and from 0.4688 to 1.7590 mPa s, respectively. The resistance of the molecular motion of the water increased, and the water diffusion decreased. The evaporation rates decreased as a result of these changes, which were not examined in previous studies of cooling towers or seawater desalination [17–19].

Based on the data provided in Table 5 and the values of β_{xv} provided in Table 4, the unknown constants in Eq. (14) were calculated using MATLAB R2010a. The results were as follows: $A = 1$, $B = -2.2560$, $C = -1.0289$, and $D = -6.1052$. Then, for the developed

Table 3
Status of the wastewater and air in the evaporation chamber

No. of sample	Air						Wastewater		
	Inlet			Outlet			Input Temperature (℃)	Return Temperature (℃)	c_w (kJ/(kg ℃))
	Temperature (℃)	Humidity (kg/kg)	Enthalpy (kJ/kg)	Temperature (℃)	Humidity (kg/kg)	Enthalpy (kJ/kg)			
1	39.0	0.0461	157.902	46.0	0.0688	224.172	59.8	53.6	4.180
2	38.3	0.0443	152.439	44.3	0.0625	205.898	59.5	54.2	3.891
3	37.7	0.0428	147.901	43.9	0.0611	201.821	59.6	54.3	3.879
4	37.1	0.0413	143.490	43.2	0.0587	194.880	59.6	54.4	3.712
5	37.2	0.0416	144.216	43.1	0.0584	193.908	59.7	54.5	3.536
6	36.0	0.0388	135.722	42.1	0.0561	184.447	59.8	54.6	3.457
7	36.1	0.0390	136.412	42.1	0.0561	184.447	59.7	54.6	3.435
8	36.0	0.0388	135.722	42.0	0.0548	183.527	59.9	54.8	3.344
9	35.9	0.0386	135.036	41.8	0.0542	181.699	59.6	54.6	3.241
10	35.8	0.0383	134.353	41.6	0.0536	179.899	59.8	54.9	3.163
11	35.7	0.0381	133.673	41.4	0.0536	178.097	59.8	55.1	3.152
12	35.6	0.0379	132.996	41.1	0.0536	175.442	59.7	55.3	3.135
13	35.5	0.0377	132.323	40.9	0.0542	173.683	59.6	55.4	3.129
14	35.3	0.0372	130.985	40.5	0.0533	170.246	59.8	55.8	3.087
15	34.9	0.0364	128.347	39.9	0.0527	165.201	59.6	55.8	3.023
16	34.9	0.0364	128.347	39.8	0.0527	164.374	59.9	56.4	3.086
17	34.9	0.0364	128.347	39.7	0.0530	163.551	59.8	56.5	3.118
18	34.9	0.0364	128.347	39.6	0.0533	162.732	59.9	56.6	2.952
19	34.4	0.0353	125.118	39.1	0.0524	158.697	59.9	56.8	2.952
20	34.3	0.0351	124.481	38.9	0.0518	157.110	59.9	56.9	2.891
21	33.0	0.0325	116.464	37.5	0.0489	146.416	59.7	57.0	2.834
22[a]	36.0	0.0388	135.722	42.3	0.0558	186.302	59.8	54.7	3.574
Pharmaceutical wastewater	35.8	0.0383	134.353	42.5	0.0564	188.175	59.9	54.7	3.481

[a]Sample no. 22 was used in the case study.

Table 4
β_{xv} values from the experiments

No. of sample	β_{xv} (kg/(m^3 h))
1	3,197.70
2	3,113.08
3	3,126.49
4	3,038.10
5	3,052.11
6	3,028.06
7	3,054.74
8	3,051.32
9	3,020.85
10	3,046.01
11	3,022.67
12	2,939.76
13	2,956.25
14	2,892.37
15	2,746.49
16	2,684.90
17	2,653.17
18	2,639.48
19	2,539.15
20	2,494.62
21	2,209.42

evaporator, Eq. (14) could be used to predict the mass transfer efficiency for the wastewater treatment process by analyzing the density, viscosity, and saturated vapor pressure of wastewater.

The test results indicated that the physical and chemical properties of the wastewater should be considered to be as important as the operating conditions and other evaporator parameters when designing the evaporation system for high-salinity wastewater treatment. When designing the proposed system, we found that the volume of the proposed system in this study was about twice as large as the volumes of other evaporation systems (MED or MVR), although the proposed system was designed to achieve the same evaporation rate as previous techniques [6,11]. Thus, more land area or a higher evaporation rate might be required to apply the proposed system.

3.3. Case study

Simulated wastewater no. 22 and a stream of real wastewater from a pharmaceutical factory were introduced into the study to verify the efficacy of the system and verify Eq. (14). The experimental results

Table 5
Characteristics data of wastewater

No. of sample	ρ (kg/m^3)	μ (mPa s)	P (kPa)
1	1,000.0	0.4688	19.90
2	1,013.3	0.7110	17.19
3	1,028.9	0.7420	16.96
4	1,043.9	0.7770	16.73
5	1,056.8	0.8120	16.52
6	1,064.7	0.8340	16.43
7	1,079.8	0.8780	16.18
8	1,094.0	0.9300	15.97
9	1,107.6	0.9830	15.80
10	1,121.3	1.0560	15.64
11	1,124.8	1.0570	15.58
12	1,134.1	1.1000	15.48
13	1,148.2	1.1680	15.32
14	1,153.7	1.2000	15.27
15	1,161.9	1.2720	15.19
16	1,173.9	1.3230	15.15
17	1,173.4	1.3260	15.11
18	1,180.1	1.3710	15.11
19	1,189.6	1.4410	15.06
20	1,195.8	1.4890	15.02
21	1,215.7	1.7590	15.01
22[a]	1,088.7	0.921	16.53
Pharmaceutical wastewater	1,081.8	0.986	16.03

[a]Sample no. 22 was used in the case study.

are shown in Table 2, the experimental properties of the wastewater and air are shown in Table 3 and the wastewater characteristics are presented in Table 5.

The removal efficiencies of TDS and COD can be as high as 99.9% for the simulated wastewater, as indicated in Table 2. For real wastewater, the removal efficiencies of TDS and COD were 99.9 and 95.8%, respectively. The high TDS removal efficiencies for simulated and real wastewater illustrated that liquid entrainment was reduced. The lower COD removal efficiency in real wastewater might be caused by the volatile organics in real wastewater. Volatile organics, such as benzene, toluene, and dichloromethane, are common pollutants in pharmaceutical wastewater, as reported by previous research [28,29]. These volatile organics could evaporate to form gasses when the wastewater was subjected to evaporation. Next, the organic gasses could be condensed to form a liquid and could mix with condensed water in the cooling chamber. Thus, the COD levels in the output were impermissibly high. However, the removal efficiency of COD reached approximately 95.8%, which indicated that the system was effective for treating high-salinity industrial wastewater.

The predicted and actual mass transfer coefficients for the simulated wastewater were 2,852.81 and 2,922.63 kg/(m^3 h), respectively. Meanwhile, the predicted and actual mass transfer coefficients for the real wastewater were 2,862.55 and 3,047.38 kg/(m^3 h), respectively. The relative difference between the predicted and actual mass transfer coefficients for the real wastewater (6.1%) was slightly larger than that for the simulated water (2.3%), likely because a portion of the volatile organics in the wastewater were evaporated with the vapor. These organics might also exist in gaseous form and accumulate in the system. Then, the saturated vapor pressure of the wastewater used to calculate β_{xv} could not accurately represent the driving force of pressure when the system reached equilibrium. Thus, the effects of volatile organics should be considered when calculating the mass transfer coefficient using Eq. (14).

The system performed well for reducing COD and TDS (>95%) in the high-salinity wastewater, and Eq. (14) was appropriate for calculating the mass transfer coefficient. However, for wastewater containing volatile organics, the COD levels in the condensed water could be impermissibly high, and post-treatment was required to ensure the quality of the output. Because most of the organics and salts pollutants can be removed, post-treatment of condensed water can easily be conducted using conventional wastewater treatment processes, such as biochemical treatment. Additional research is required to determine the complex migration processes of volatile organics in this system.

4. Conclusions

In this study, a small evaporation system with a 5 L/h capacity was operated at low temperature and ambient pressure to investigate its efficacy for treating high-salinity wastewater. The results of this study led to the following conclusions.

The system exhibited good performance for wastewater treatment, especially for high-salinity wastewater. The COD and TDS removal efficiencies were as high as approximately 99.9%. Additionally, the wastewater could be sufficiently concentrated to achieve solid precipitation. In addition to the operating conditions and evaporator characteristics, the physical and chemical properties of the wastewater significantly affected the evaporation rate. All of these factors should be considered when designing the evaporation system based on direct contact between wastewater and air for wastewater treatment. In the proposed system, the pump, fan, and heating section account for most energy expenses, with no other energy required during the process. Therefore, the developed evaporation system, which operates at low temperature and ambient pressure, is economically feasible and is promising for treating high-salinity industrial wastewater.

Acknowledgements

The authors gratefully acknowledge the financial support from the National Natural Science Foundation of China (grant number 50978118). The authors are thankful to Dr Shuang Tong, at China University of Geosciences (Beijing) and Dr Samuel Ma, at Texas A&M University for their technical assistance.

Nomenclature

a'	—	specific surface area of the fillers (m^2)
c_w	—	specific heat of the wastewater (kJ/(kg °C))
d	—	spacing between two filler plates (m)
D_P	—	diffusion coefficient based on the pressure difference (m^2/s)
g	—	mass flow rate of the air (kg/h)
G	—	volumetric flow rate/cross sectional area of the air (m/s)
h_1	—	enthalpy of the inlet air (kJ/kg)
h_2	—	enthalpy of the inlet air (kJ/kg)
h_m	—	average value of h_1 and h_2 (kJ/kg)
h_1'	—	enthalpy of the saturated air at the temperature of the input water (kJ/kg)

h'_2 — enthalpy of the saturated air at the temperature of the return water (kJ/kg)
h'_m — average value of h'_1 and h'_2 (kJ/kg)
K — the correction factor for the amount of water evaporated
n — number of filler plates
P — saturated vapor pressure (kPa)
q — mass flow rate of the wastewater (kg/h)
$r(T)$ — latent heat of vaporization of the wastewater when the temperature is T
R_{ws} — gas vapor constant
S — cross sectional area (m^2)
T — temperature of the wastewater (℃)
T_1 — temperature of the return wastewater (℃)
T_2 — temperature of the inlet wastewater (℃)
U — relative velocity between the air and wastewater (m/s)
U_L — velocity of the air (m/s)
U_W — velocity of the wastewater (m/s)
V — filler volume (m^3)
x_1 — inlet air humidity (kg/kg)
x_2 — outlet air humidity (kg/kg)
β_{xv} — volumetric mass transfer coefficient (kg/(m^3 h))
β_P — area mass transfer coefficient based on the pressure difference (kg/(m^2 h))
ρ — wastewater density (kg/m^3)
μ — wastewater viscosity (mPa s)

References

[1] M. Xie, Z. Liu, Y. Xu, Removal of glyphosate in neutralization liquor from the glycine-dimethylphosphit process by nanofiltration, J. Hazard. Mater. 181 (2010) 975–980.
[2] G. Parthasarathy, R.F. Dunn, Graphical strategies for design of evaporation crystallization networks for environmental wastewater applications, Adv. Environ. Res. 8 (2004) 247–265.
[3] A. Fakhru'l-Razi, A. Pendashteh, L.C. Abdullah, D.R.A. Biak, S.S. Madaeni, Z.Z. Abidin, Review of technologies for oil and gas produced water treatment, J. Hazard. Mater. 170 (2009) 530–551.
[4] I. Freuze, A. Jadas-Hecart, A. Royer, P.-Y. Communal, Influence of complexation phenomena with multivalent cations on the analysis of glyphosate and aminomethyl phosphonic acid in water, J. Chromatogr. A 1175 (2007) 197–206.
[5] G. Raluy, L. Serra, J. Uche, Life cycle assessment of MSF, MED and RO desalination technologies, Energy 31 (2006) 2361–2372.
[6] D. Zhao, J. Xue, S. Li, H. Sun, Q. Zhang, Theoretical analyses of thermal and economical aspects of multi-effect distillation desalination dealing with high-salinity wastewater, Desalination 273 (2011) 292–298.
[7] O. Lefebvre, R. Moletta, Treatment of organic pollution in industrial saline wastewater: A literature review, Water Res. 40 (2006) 3671–3682.
[8] A.D. Khawaji, I.K. Kutubkhanah, J.-M. Wie, Advances in seawater desalination technologies, Desalination 221 (2008) 47–69.
[9] I.C. Karagiannis, P.G. Soldatos, Water desalination cost literature: Review and assessment, Desalination 223 (2008) 448–456.
[10] K. Ranganathan, K. Karunagaran, D. Sharma, Recycling of wastewaters of textile dyeing industries using advanced treatment technology and cost analysis—Case studies, Resour. Conserv. Recycl. 50 (2007) 306–318.
[11] T.D. Hayes, B. Halldorson, P.H. Horner, J.J.R. Ewing, J.R. Werline, B.F. Severin, Mechanical vapor recompression for the treatment of shale-gas flowback water, Oil Gas Facil. 3 (2014) 54–62.
[12] K.C. Ng, K. Thu, Y. Kim, A. Chakraborty, G. Amy, Adsorption desalination: An emerging low-cost thermal desalination method, Desalination 308 (2013) 161–179.
[13] K. Thu, K.C. Ng, B.B. Saha, A. Chakraborty, S. Koyama, Operational strategy of adsorption desalination systems, Int. J. Heat Mass Transfer 52 (2009) 1811–1816.
[14] N. Ghaffour, S. Lattemann, T. Missimer, K.C. Ng, S. Sinha, G. Amy, Renewable energy-driven innovative energy-efficient desalination technologies, Appl. Energy 136 (2014) 1155–1165.
[15] S. Shelley, Device and method for utilising surplus cooling of water in a cooling tower, US 20110011107 A1, Patents, 2009.
[16] S. Shelley, Fluid fractionation process and apparatus, US 8591704 B2, Patents, 2013.
[17] J.F. Klausner, Y. Li, R. Mei, Evaporative heat and mass transfer for the diffusion driven desalination process, Heat Mass Transfer 42 (2006) 528–536.
[18] M. Lemouari, M. Boumaza, A. Kaabi, Experimental analysis of heat and mass transfer phenomena in a direct contact evaporative cooling tower, Energy Convers. Manage. 50 (2009) 1610–1617.
[19] K. Bourouni, M.T. Chaibi, L. Tadrist, Water desalination by humidification and dehumidification of air: State of the art, Desalination 137 (2001) 167–176.
[20] S. Al-Hallaj, M.M. Farid, A.R. Tamimi, Solar desalination with a humidification-dehumidification cycle: performance of the unit, Desalination 120 (1998) 273–280.
[21] G.F. Cortinovis, M.T. Ribeiro, J.L. Paiva, T.W. Song, J.M. Pinto, Integrated analysis of cooling water systems: Modeling and experimental validation, Appl. Therm. Eng. 29 (2009) 3124–3131.
[22] M.K. Mansour, M.A. Hassab, Innovative correlation for calculating thermal performance of counterflow wet-cooling tower, Energy 74 (2014) 855–862.
[23] Q. Zhang, J. Wu, G. Zhang, J. Zhou, Y. Guo, W. Shen, Calculations on performance characteristics of counterflow reversibly used cooling towers, Int. J. Refrig. 35 (2012) 424–433.
[24] K.K. Chan, M.W. Golay, Comparative Evaluation of Cooling Tower Drift Eliminator Performance, PhD Thesis, MIT Energy Laboratory, Massachusetts Institute of Technology, Cambridge, MA, 1977.
[25] M. Lucas, P.J. Martínez, A. Viedma, Experimental determination of drift loss from a cooling tower with different drift eliminators using the chemical balance method, Int. J. Refrig. 35 (2012) 1779–1788.
[26] R. Saidur, E.T. Elcevvadi, S. Mekhilef, A. Safari, H.A. Mohammed, An overview of different distillation methods for small scale applications, Renew. Sustain. Energy Rev. 15 (2011) 4756–4764.

[27] G.v. Houwelingen, R. Bond, T. Seacord, E. Fessler, Experiences with pellet reactor softening as pretreatment for inland desalination in the USA, Desalin. Water Treat. 13 (2010) 259–266.
[28] V.S. Priya, L. Philip, Treatment of volatile organic compounds in pharmaceutical wastewater using submerged aerated biological filter, Chem. Eng. J. 266 (2015) 309–319.
[29] C.S. Slater, M. Savelski, A method to characterize the greenness of solvents used in pharmaceutical manufacture, J. Environ. Sci. Health, Part A 42 (2007) 1595–1605.